PHYSICS AND CHEMISTRY OF SOLID STATE
V. 27, No. 1 (2026) pp. 74-85
Section: Technology

DOI: 10.15330/pcss.27.1.74-85

Vasyl Stefanyk Carpathian National University

ФІЗИКА І ХІМІЯ ТВЕРДОГО ТІЛА
Т. 27, № 1 (2026) С. 74-85
Технічні науки

74

PACS: 81.20.Ka

ISSN 1729-4428 (Print)
ISSN 2309-8589 (Online)

Ravi Shankar Rai[1*], Ruby Pant[2], Shristi Chaudhary[3], Rupesh Gupta[4], Chandrmani Yadav[5]

Synthesis and characterizations of ZnO nanoflowers prepared by one step microwave assisted solvothermal route for optoelectronic applications

[1]Department of Automation and Robotics, JSPM's Rajarshi Shahu College of Engineering, Pune, Maharashtra, India, rash.mait@gmail.com;
[2]Department of Mechanical Engineering, Uttaranchal University, Dehradun, Uttarakhand, India;
[3]University Centre of Research and Development, Chandigarh University, Gharuan, Punjab, India;
[4]Chitkara University Institute of Engineering and Technology, Chitkara University, Punjab, India;
[5]Marwadi University Research Center, Faculty of Engineering & Technology, Department of Mechanical Engineering, Marwadi University, Rajkot, Gujarat, India

In this study, blossom-shaped ZnO nanoflowers (NFs) were successfully synthesized using a rapid, one-step microwave-assisted solvothermal method with zinc nitrate hexahydrate and hexamethylenetetramine as precursors. The synthesis was completed within five minutes, relying solely on inexpensive reagents and eliminating the need for costly additives or high-temperature furnaces, thereby providing an efficient and economical route. Structural analysis through X-ray diffraction confirmed the high crystallinity of the ZnO NFs, while field emission scanning electron microscopy revealed their characteristic blossom-like morphology with an average particle size of approximately 18 nm. Optical properties were investigated by UV–visible spectroscopy, where a sharp absorption peak near 348 nm indicated good monodispersity. The optical band gap was determined as 3.22 eV using Tauc's relation, which is significantly lower than that of bulk ZnO (3.51 eV), demonstrating a red shift. Moreover, the computed Urbach energy of 0.34 eV reflects low structural disorder in the nanostructures. The combination of rapid synthesis, controlled morphology, high crystallinity, and favorable optical characteristics underscores the novelty and strong potential of these ZnO nanoflowers for future optoelectronic and photonic device applications.

Keywords: Microwave, Solvothermal method, Synthesis, Characterization, ZnO, Nanoflowers, Opto-electronics.

Receive 08 October 2024; Accepted 03 February 2026.

Introduction

Due to its essential electrical and optical properties, which are very useful in developing Nano-scaled optoelectronic and electronic appliances, there has been an increasing interest in the creation of Nano-sized semiconductors over the past few years [1–3]. ZnO, one of many semiconducting materials, has a wide energy band of 3.37 eV and a high binding energy (60 meV) at atmospheric conditions, making it a promising electrical and photonic material [4,5]. The use of ZnO in mechanical actuators and piezoelectric sensors is a result of the solid piezoelectric and pyroelectric properties of wurtzite, which are caused by the absence of a focal point of symmetry and a significant electromechanical connection [6–8]. ZnO is an expected contender for optoelectronic usages in narrow wavelength range as it shows comparative features to GaN so that ZnO can also make heterojunctions for varied applications [9–11]. The nanostructures (NSs) of ZnO are potential material classification to investigate due to their affluence of NSs development, assorted morphologies other than being a significant multifunctional material displaying extraordinary optoelectronics features much needed for diverse appliances like sensors, catalysts, emitters and biomedical agents [12–14]. There are several ways to

make ZnO NSs, and they can all use either of the two common techniques, the aqueous method or the vapor method [15–17]. Out of these, the aqueous approach is more ideal due to its many benefits, including affordability, ease of growth, low temperature, and high purity [18,19]. Because it features minimal aggregation, narrow particle dispersion, and a two-step procedure (seeding and growth), the hydrothermal method is an enhanced variation of the wet chemical method that offers superior NSs synthesis [20–22]. Additionally, using this technique, pure NSs with superb morphologies and manageable sizes can be created [23,24]. For the growth of NSs, microwave heating has become more appealing than conventional heating in recent years, and microwave assisted growth is highly quick and single step growth of NSs. Thus researchers started using microwave assisted hydrothermal growth model for the development of advance materials because of following advantages [25].

Uniform and controlled volumetric heating causes homogenous nucleation and development of ZnO NSs in short duration,

Minimum power consumption for the NSs growth due to microwave irradiation.

There is a wealth of literature on the production of ZnO NSs using hydrothermal procedures with microwave assistance [25,26], but little research has been done on the effects of synthesis parameters on the properties of produced NSs [27–29]. Ahammed et al. [30] successfully synthesized ZnO nanoparticles of spherical shape having average particle size of 70-90 nm. They have used poly vinyl alcohol, ascorbic acid and their combinations to synthesize nanoparticles which are expensive chemicals. The overall duration to synthesize nanoparticles in this case is higher and also requires high temperature furnace (500 °C) in comparison to simple hot air furnace of 100-150 °C temperature range. Mesut Yalcin [31] applied microwave assisted method to develop ZnO nanoflakes have been having crystallite size of 33.8 nm. They have also used high temperature furnace for drying of the nanopowders that subsequently increases overall cost of production. Sharma et al. [32] prepared zinc oxide nanoparticles using a facile route which is based on the addition of zinc sulphate heptahydrate and NaOH in dropwise manner amalgamation in air, sudden amalgamation in air and using microwave radiations. They achieved nanochip, bipodal and spherical morphologies of ZnO nanoparticles. Al-Gaashani et al. [33] prepared ZnO nanostructures of varied morphologies such as nanoparticles, NFs and nanorods by microwave-assisted solution based method. They have used additives such as pyridine in a drop-wise manner to control the ZnO morphology which increases setup cost and chemical precursor cost. Thus it can be say that, very few researchers achieved NF-like morphologies of ZnO nanoparticles using expensive chemical precursors and advanced set up that subsequently increases overall production cost. However current work achieved NF-like morphologies of ZnO in a short duration using basic Zn-based chemical compounds and low setup which is difficult to synthesize by other processes such as hydrothermal process, sol-gel process and vapor deposition techniques. While microwave-assisted hydrothermal methods have been reported, most studies either required expensive surfactants, complex additives, or extended processing times. Moreover, NF-like morphologies are rarely achieved in a reproducible, low-cost, and ultrafast manner. In contrast, the present work demonstrates for the first time the synthesis of blossom-like ZnO nanoflowers in just 5 minutes using only zinc nitrate hexahydrate and HMTA as precursors, combined with low-temperature drying. This cost-effective and energy-efficient route yields nanoflowers with reduced crystallite size (~18 nm), a narrowed band gap (3.22 eV), and low Urbach energy, providing a new pathway for scalable production of ZnO nanostructures tailored for optoelectronic applications.

Current study deals with the synthesis of blossom shaped ZnO nanoparticles using microwave assisted hydrothermal phenomenon. This study examines how microwave power and synthesis time affect the creation of ZnO NSs that resemble NFs. Microwave heating of the growth medium produced for ZnO caused the combination of various nanopetals and nanorods to take on the shape of a flower. The generated NFs have outstanding optical qualities and a good crystalline structure, which are required for optoelectronic applications. The computation of Urbach energy was used to determine the micro-structural lattice disorder, and the resultant value shows that disorder exists in the material.

I. Materials and methodology

1.1. Materials

In this experimentation different chemical of analytical grade was used. The preparation of ZnO NFs was done with the help of Zinc nitrate hexahydrate (ZNH), hexamethylene-tetraamine (HMTA) ethanol and deionized water. Without additional purification, the chemicals that were purchased were used.

1.2. Preparation of ZnO NFs

HMTA and ZNH created zinc oxide NFs using the microwave aided hydrothermal method in deionized water, and ethanol was used to clean the finished product. Equi-molar proportions of HMTA and ZNH were combined with deionized water to provide a growth solution of 30 mM for the growth of ZnO NSs. 30 mM of HMTA was added to the 300 ml of aqueous deionized water solution after 30 mM of ZNH had been dissolved in it. The solution was then stirred using a magnetic stirrer for another 30 minutes to prepare the final 300 ml of deionized water. After 30 minutes of vigorous stirring, the HMTA solution was dropped-by-drop blended with the ZNH solution.

Now, after vigorous stirring, the produced HMTA solution was dropped-by-drop combined with the ZNH solution. The resulting mixture was stirred for another 40 minutes to ensure that ZNH and HMTA were completely dissolved in ethanol. After the final solution had been sealed under atmospheric conditions for 15 minutes, a household microwave (model Samsung-QW71X, frequency 2.45 GHz, max power 1600 W) was used to illuminate the precursor solution at a microwave power set of 1000 W for 5mins. The $\{Zn(NH_3)_4^{2+}\}$ and OH^- exist in the solution started producing ZnO NFs because of the

microwave irradiation as a result the photon energy of the microwave is adequately low and only having an impact on kinetic atomic excitation. The solution that resulted from the microwave treatment was allowed to cool at room temperature so that the NFs would drop to the bottom of the flask. The solution is then centrifuged to improve precipitate filtration. The precipitates were collected in a petri dish and repeatedly cleaned with a mix of ethanol and deionized water to remove impurities and byproducts. The produced ZnO NFs underwent a 4-hour, 70°C hot air oven drying process. The ZnO NFs are exposed to air conditions for a few hours, allowing zinc hydroxide to completely dry up and change into ZnO [34]. The reproducibility of the synthesis was confirmed by repeating the microwave-assisted synthesis five times under identical conditions. All batches consistently produced blossom-like ZnO NFs with crystallite sizes between 17-19 nm, absorption maxima at 348 ± 2 nm, and band gap values of 3.22 ± 0.05 eV. This demonstrates the reliability of the proposed synthesis route for large-scale production. In Fig. 1, the entire process of creating ZnO NFs is depicted. Utilizing the W-H Plot method and X-ray diffraction methodology, produced NSs were analyzed. ZnO NFs' morphology was studied using field emission scanning electron microscopy (FESEM). By using UV-vis spectroscopy, optical properties of manufactured NFs were analyzed, and the effects of absorption, absorption coefficient, and Urbach energy were examined.

II. Results and Discussion

2.1. X-ray diffraction

An X-ray diffractometer with Cu-K radiation is utilized to analyze the produced structure and crystal behavior of ZnO NFs. In Fig. 2, the prepared ZnO NSs' XRD peaks are depicted. The XRD graph supported the hexagonal wurtzite phase of ZnO NSs. The crystal of wurtzite, which has the chemical formula ZnO and a hexagonal crystal system with the space groups P63 m c and 186, makes up the developed structure.

For the study of the grown structure and crystal behavior of ZnO NFs, an X-ray diffractometer containing Cu-K radiation is utilized. Figure 2 depicts the XRD peaks of prepared ZnO NSs. The XRD graph confirmed the hexagonal wurtzite phase of ZnO NSs. The resulting structure is a wurtzite crystal with the chemical formula ZnO and a hexagonal crystal system with space groups P63 m c and 186. The produced ZnO's crystal properties are a = b = 3.25, c = 5.20, and = 90°; =120°. ZnO NFs generated on planes bearing (hkl) values (100), (002), (101), (102), (110), (103), (200), (112) and (201) indexed to angular position of 31.52°, 34.32°, 36.21°, 47.46, 56.49°, 62.89°, 66.28°, 67.94° and 69.10° correspondingly are in match with the JCPDS database No: 36-1461. Out of these peaks the pure wurtzite crystal structure of ZnO lies on hkl planes of (100), (002), (101), (102), (110) and (200) coincide with 2θ value of 31.52°, 34.32°, 36.21°, 47.46, 56.49° and 67.94° respectively. Some of the zincite crystal structure having chemical formula Zn_2O_2 was developed corresponding to hkl values of (103), (112) and (201) indexed to angular position of 62.89°, 68.28° and 69.10° respectively coincide with JCPDS database No: 36-1461. The zincite crystals were formed by oxidation of zinc ions in presence of carbon di-oxide during the drying of the ZnO NFs inside the hot air oven. Zincite is a rather uncommon natural oxide of zinc having chemical formula is ZnO. Crystals of zincite are extremely rare and typically quite tiny. The following reactions indicate that in an oxidizing environment, contact of the zinc vapour with ambient CO_2 led to a rapid formation of evidently primary zincite crystals [35]:

$$Zn(g) + CO_2 \leftrightarrow ZnO(s) + CO$$

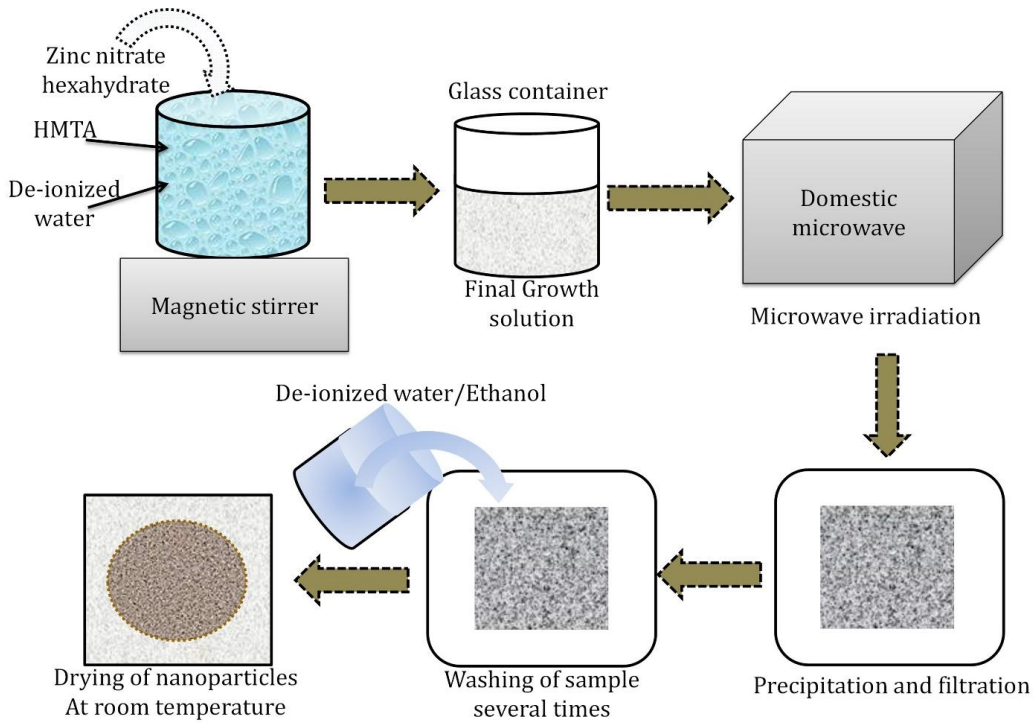

Fig. 1. Synthesis of ZnO NFs via microwave based hydrothermal technique.

$$Zn(g) + {}^{1}/_{2}\,O_2 \leftrightarrow ZnO(s)$$

The discovery of a few more ZnO NF peaks led to further analysis, which revealed the development of another ZnO compound with Wuelfingite crystals with the chemical formula Zn4O8. The crystal system, which is orthorhombic and belongs to the space group P 21 21 21, has the following crystal parameters: a=4.92, b=5.16, c=8.53 A°, and ===90°. The developed NFs on the planes with the (hkl) values (111), (102), (112), (020), (201), (120), (121), (211), (202), (212), (114), (221), (031), (301), (131), (124) and (302) are indexed to angular positions of 27.12°, 27.65°, 32.73°, 34.74°, 38.03°, 39.4°, 40.85°, 42.01°, 42.38°, 44.97°, 46.04°, 49.81°, 52.46°, 54.37°, 57.14°, 57.75°, 59.22° and 60.42° respectively based on JCPDS database No-96-101-1224. Due to the quick microwave irradiation of the precursor solution and post-annealing of the resultant nanopowders produced by the microwave aided hydrothermal synthesis approach, these are essentially anharmonic thermal vibrations in ZnO [36].

Out of the developed zinc oxide crystals, the peaks corresponding to ZnO wurtzite crystal structures are the targeted compound of the current study. Remaining compounds were observed by detailed study of the XRD data using X'pert high score software. Further analysis for the calculation of particle size, crystallite size and strain were performed based on the highest peak of the wurtzite phase of ZnO. The diameter of synthesized ZnO NFs was derived from Debye-Scherrer expression [29];

$$D = \frac{K\lambda}{\beta_D cos\theta}$$

Where K is the Scherrer's constant (often K=0.9), X-ray wavelength, Bragg diffraction angle, and full width at half-maximum (FWHM) of the diffraction spectrum along the (101) plane are given. By using Scherrer's relation, the average particle size along (101) plane at 36.21° is calculated using the value. Therefore, using this method, the average particle size is roughly 17 nm. The Williamson-Hall expression was used to determine the strain due to crystal defect using the W-H plot of the diffraction peak [37]:

$$\varepsilon = \frac{(\beta_{hkl})}{4\,tan\theta}$$

As shown in Fig. 3, the W-H plot is a graphical depiction of the variation of (4 sinθ) and (β_t cosθ), which correspond to the x- and y-axes, respectively. The intercept on the y-axis will provide the value for crystallite size, while the slope of the graph will provide the value for strain 'ε'. The strain " value will be used to indicate the line's gradient, and the size of the crystallites will be determined from the y-intercept '$\frac{K\lambda}{D}$'. As a result, the W-H plot shows that the crystallite size is "18.64 nm" and the strain value is "0.842 × 10^{-3}". Hooke's law ($\sigma = E\varepsilon$), can be used to determine the system's stress value. "E" stands for the system's bulk Young's modulus, which is equal to '1.46×10^{10} N/m^2', the particle's strain is 'ε', and 'σ' for the system's stress. Thus, the ZnO NFs' strain and stress were determined to be equal to '0.842 × 10^{-3}' and '12.3 MPa'.

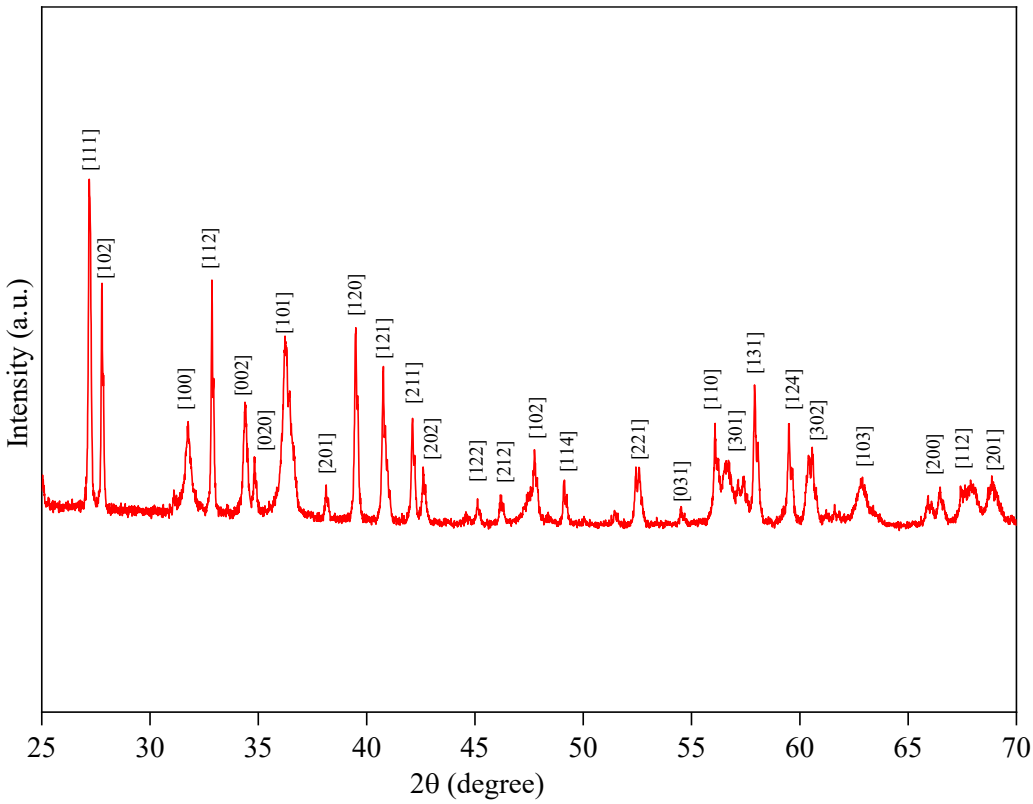

Fig. 2. XRD spectra of different crystals of as prepared ZnO NFs.

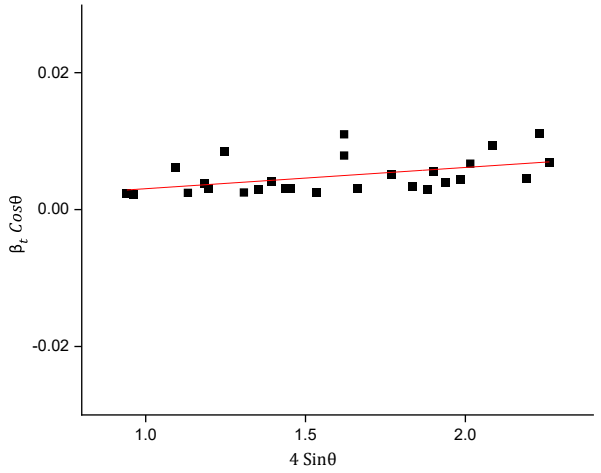

Fig. 3: W-H plot of as synthesized crystalline ZnO NFs.

2.2. Morphological study of synthesized ZnO NFs

The FESEM investigations were used to characterize the morphology of synthesized ZnO NFs. According to the FESEM image in Fig. 4, which is magnified in the inset at a magnification of 60 KX and 200 nm size, the produced nanoparticles have a nanostructure resembling flowers. This micrograph shows that ZnO NFs have formed. The micrograph supports the ZnO NSs' blossom-like structure, with all of the petals displaying some carving. ZnO nanoparticles took on the appearance of a flower after being microwave heated and then cooled to room temperature by merging various nanopetals and nanorods. Using image-J software to analyze a FESEM image, the size of ZnO NSs was calculated. The average size of a NF is determined to be in the region of 580 nm, with the average size of each petal being about 260 nm. The Scherrer's expression for XRD peaks demonstrates that the calculated particle size by NF is consistent with the smallest size of NF, which is found to be in the region of 18 nm.

2.3. Compositional analysis of synthesized ZnO NFs

The Fig. 5 illustrates composition of the generated ZnO NFs as well as the results of the energy-dispersive X-ray spectroscopy (EDS) spectra. Quantitative analysis reveals that Zn and O are present in a 1:1 stoichiometric ratio, and the EDS spectra amply demonstrated the presence of Zn and O atoms. The one-step chemical bath deposition of ZnO using microwave heating and the presence of zinc and oxygen elements in the produced growth solution indicate the development of ZnO at the nanoscale. ZnO NFs can be used to produce novel nanomaterial for a range of photonics and optoelectronic industries once they have been proven. Compared to previously reported ZnO nanostructures synthesized by microwave-assisted or hydrothermal methods [30–33], our approach offers a unique combination of ultrafast processing (5 min vs. several hours), low crystallite size (~18 nm vs. 33–90 nm), and morphology control without costly surfactants or high-temperature furnaces. These advantages make the present method more cost-effective, scalable, and energy-efficient for ZnO NF synthesis.

2.4. Optical characterization by UV-Vis spectrophotometer

Absorption graph of ZnO NFs

The crystallite size has a considerable impact on the overall ZnO NSs properties. In this way, research into and expansion of ZnO NSs' size as a semiconductor material prove crucial for analyzing the material's characteristics. The most common method for understanding the optical properties of ZnO NFs is to use a UV-vis spectrophotometer to analyze the absorption spectra, as Figure 6 illustrates. There is a noticeable shift in the absorption spectra around 348 nm, which suggests the presence of ZnO NFs. This wavelength value is shorter

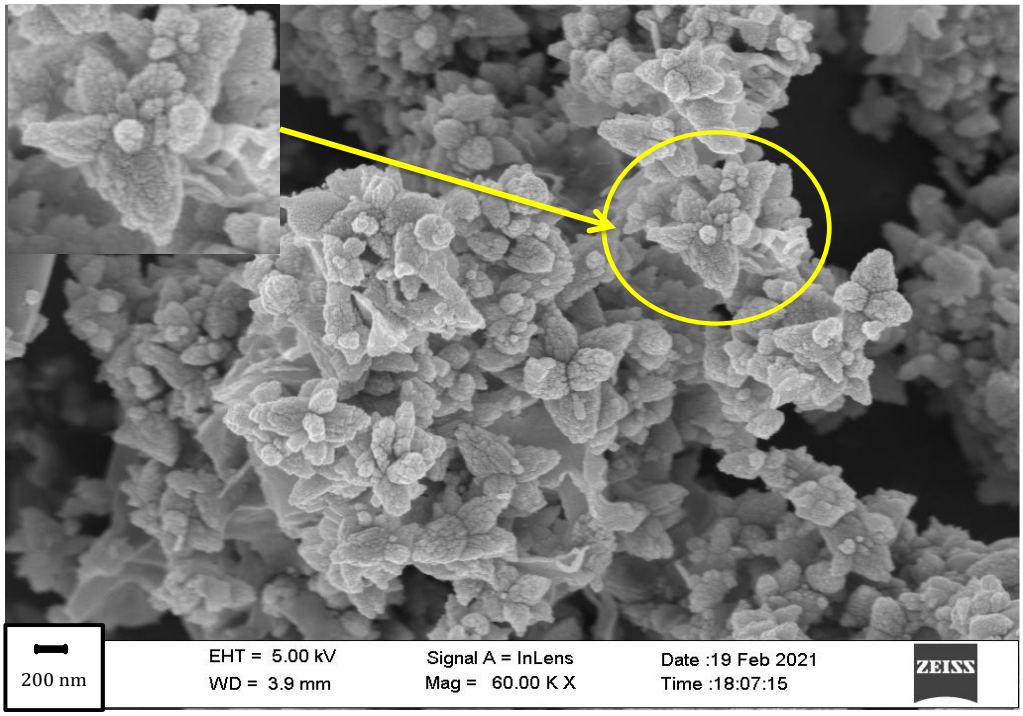

Fig. 4. An enlarged view of the synthesized ZnO nanoparticles' NF shape is provided in the inset of this FESEM image.

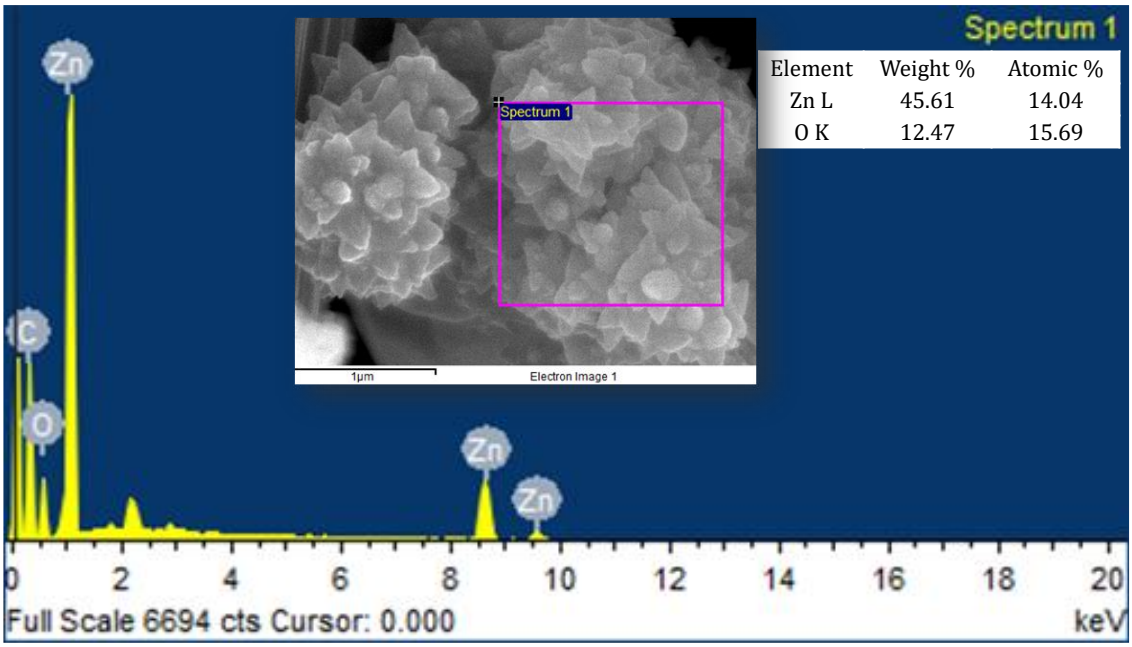

Fig. 5. Energy-dispersive X-ray spectroscopy spectra of as synthesized ZnO NFs.

than the wavelength that corresponds to the energy band gap of ZnO (Eg = 3.51 eV), which is wavelength (353 nm). This abrupt absorption caused by ZnO NFs clearly demonstrates the NFs' monodispersion [37]. Finally, the energy band gap value of the ZnO NFs is calculated using Tauc's formula of optical characterization as [38]:

$$(\alpha h\nu) = B(h\nu - E_g)^n$$

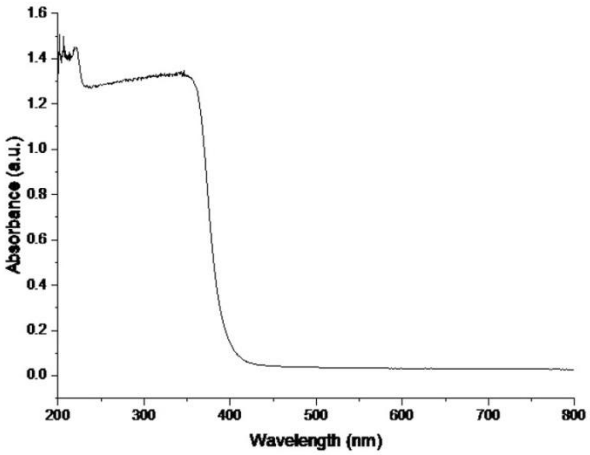

Fig. 6. Absorption spectra of ZnO NFs.

Where, B is a material-dependent constant, hυ is referred to as the photon energy, E_g is the energy band gap, α is referred to as absorption coefficient and n represents the type of transition (in this example, n = ½, which is a direct transition). Thus, using the Tauc's plot as shown in Fig. 7, it is possible to determine the direct energy band. By extrapolating from the Tauc's plot, the derived value of the energy band is roughly 3.22 eV, which is less than the band gap value of bulk ZnO (3.51 eV) [39]. The band gap value is 0.29 eV different from pure ZnO, which may be the result of post-annealing in a hot air oven following microwave treatment. Due to quantum confinement, which may exist as a result of flaws or vacancies in the inter-granular zone, the wavelength of the resultant material has shifted slightly towards the red, raising the energy level of the ZnO NFs. This behavior of ZnO NFs in their as-prepared state suggests that the material has the potential to be used in optoelectronics sectors [6,27].

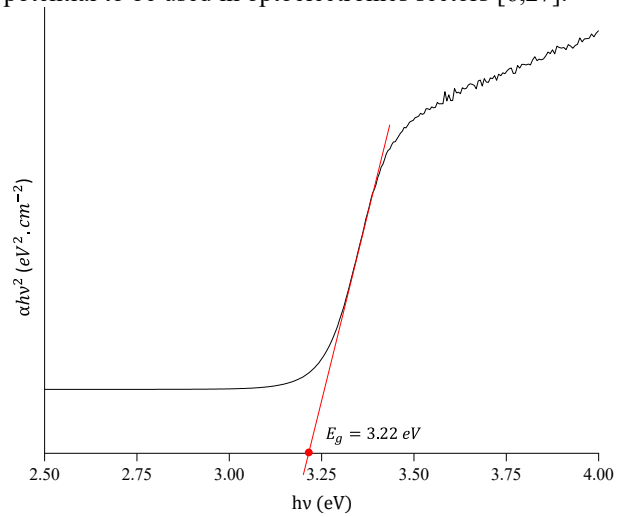

Fig. 7. Band gap calculation of ZnO NFs by Tauc's plot method.

Study of absorption coefficient

The material's optical behavior is significantly influenced by the coefficient of absorption (α). It deals with the relationship between incident radiation and the specimen's length along the wave's path. According to the following expression, absorption coefficient and absorbance value are related [38]:

$$\alpha = 2.303\ \frac{A}{d}$$

Figure 8 illustrates how the ZnO NFs' coefficient of absorption changes with photon energy. Coefficient of

absorbance depends on the scan wavelength since photon energy is related to wavelength. From the graph, it is clear that the absorption is lowest at low wavelengths and gradually increases with rising wavelengths, just like in semiconductors. It is obvious that crystalline samples exhibit better when a small absorption peak is present [40]. The crystalline structure of metal-oxides is preferred for optoelectronic applications, which is obtained in this work; therefore, it can be concluded that this kind of variation indicates the viability of using ZnO NFs for semiconductor device applications [40–43].

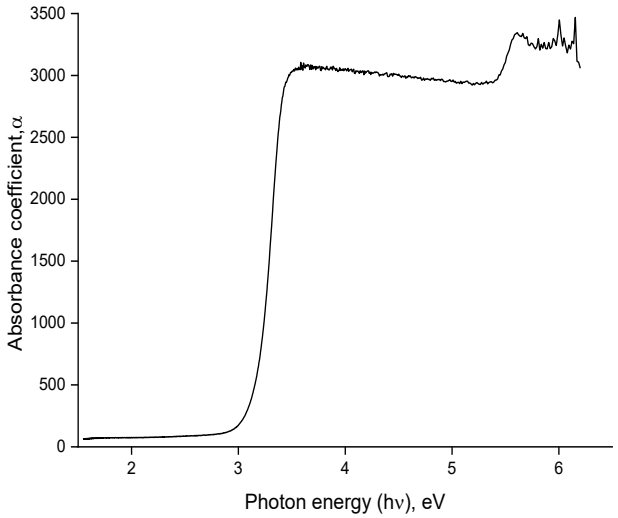

Fig. 8. Behavior of coefficient of absorption of ZnO NFs as a function of wavelength.

2.5. Urbach energy

The amount of Urbach energy associated with the prepared ZnO NFs is calculated in order to examine their disorder. The conversion of the localized conduction band and the enlarged valence band is what determines the Urbach energy value [44]. The magnitude of the localized state of the band in the energy band is another definition of the Urbach energy. Therefore, the fluctuation in the coefficient of absorption can be used to determine the level of disorder in the ZnO NFs. The following expression can be used to define Urbach energy in the region of ($h\upsilon < E_g$) [44];

$$\alpha = \alpha_0 \exp\left\{\frac{h\upsilon}{E_u}\right\}$$

Where 'E_u' is the Urbach energy, and α_0 is a constant. The Urbach energy can be determined from the graph of the logarithmic fluctuation of absorption coefficient as a function of wavelength by estimating the reciprocal of the slope of the linear component of the graph, as illustrated in Figure 9. The Urbach energy in this instance is 0.34 eV, demonstrating the presence of disorder in the material in conjunction with lattice disorder in the microstructure. Urbach energy is predicted to be 0.34 eV. The values demonstrate that this hybrid chemical has disorder. In actuality, the disorder of the microstructural lattice is related to the Urbach energy.

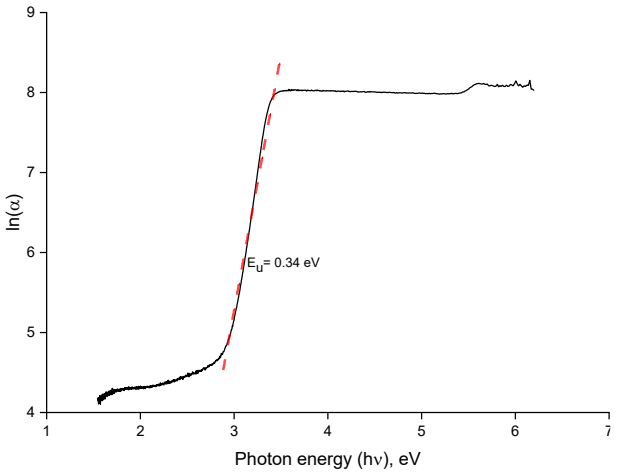

Fig. 9. Urbach energy is illustrated by the logarithmic fluctuation of the absorption coefficient of ZnO NFs with photon energy.

2.5. Optical conductivity study of ZnO NFs

Optical conductivity is a crucial material characteristic that connects the current density to the electric field at standard frequencies. High-frequency electrical transport that has been changed is known as optical conductivity. An essential property that characterizes a material's optical properties and is used to identify its permitted inter-band optical transitions is optical conductivity ($\sigma_{opt.}$). It is a quantitative, non-contact test with a tendency towards charged results. The material's optical conductivity is calculated using the following expression [45]:

$$\sigma_{opt.} = \frac{\alpha n c}{4\pi}$$

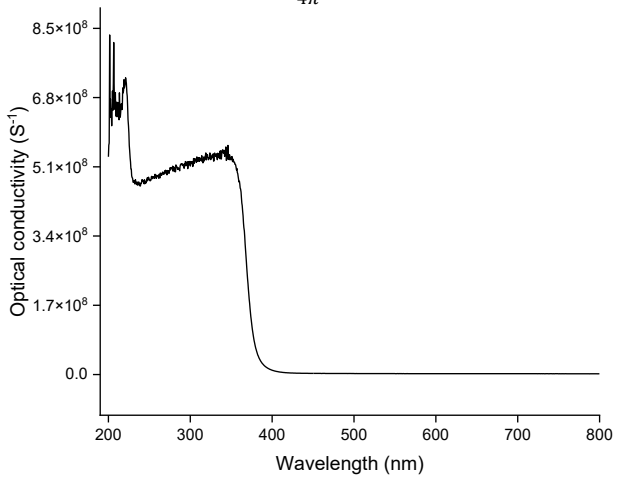

Fig. 10. Variation of Optical conductivity of produced ZnO NFs with wavelength.

Where the letters, n, and c stand for the absorption coefficient, refractive index, and vacuum light speed, respectively. Figure 10 illustrates how microwave heating of the precursor solution in the visible wavelength range alters the optical conductivity of the resulting ZnO NFs. The conductivity plot of ZnO reveals their distinctive characteristics. Due to the activation of electrons during interactions with photons, the graph shows a nonlinear relationship between optical conductivity's ($\sigma_{opt.}$) behaviour and photon energy. The optical conductivity of

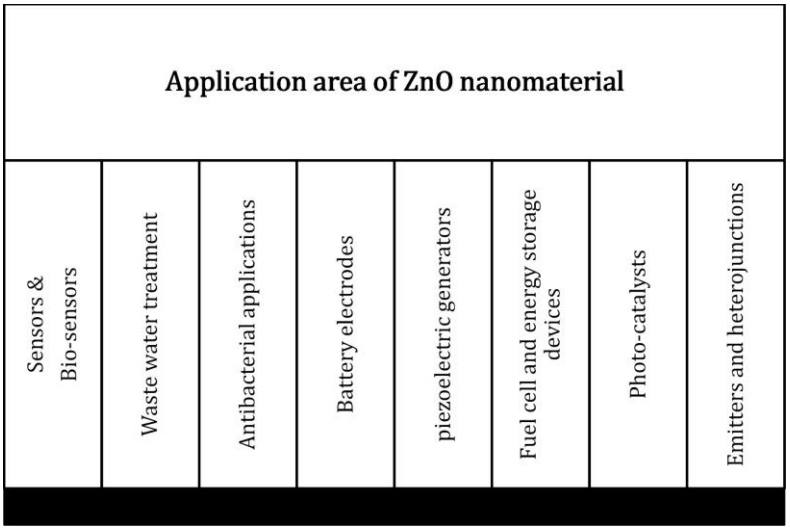

Fig. 11. Scopes to utilize developed ZnO nanomaterial [14].

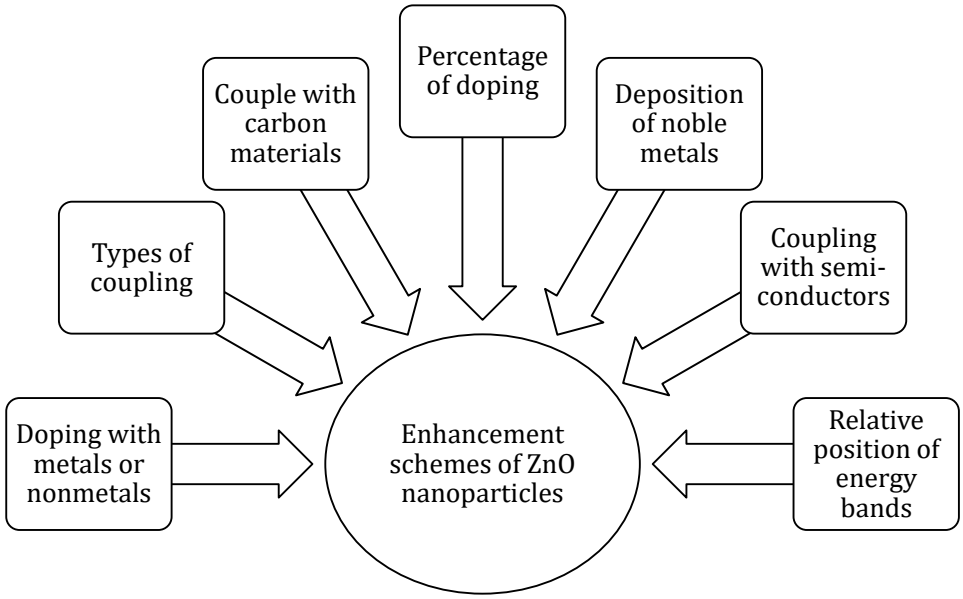

Fig. 12. Schemes to developed enhanced features of ZnO nanomaterial [14].

NFs exhibits erratic change in conductivity value before 250 nm wavelength and then grows linearly until 360 nm wavelength, but then lowers rapidly beneath the band gap area before becoming constant due to the floral structure of ZnO under their optical band gap. The graph's linear part provides a good explanation for ZnO's optical conduction at its pure ZnO energy level.

III. Potential Applications

The main uses of ZnO 3D layered constructions include photocatalysis, field emission, electrochemical sensors, antibacterial activities, and electrodes for lithium ion batteries [46–48]. Studies are currently being done on how to use ZnO nanostructures' distinctive properties to create high-performance composite materials. Some of these composites' most well-known applications are in the aviation sector 48 because of their improved mechanical properties, particularly impact strength. Applications in the domains of robotics and artificial intelligence, sensors and biomaterials, microelectronics and photonics, as well as military and artillery, will benefit from ongoing advancements in these materials [49,50]. Recent developments in the production of ZnO nanostructures on carbon fibers resulted in an extensive variety of potential uses in comparison to natural fibers [51,52]. Because of their advanced level of development in compared to their metal and ceramic equivalents, as well as their unique properties, polymer-based nanocomposites are at the forefront of applications [53,54]. The potential applications of ZnO-based nanomaterial are shown in Figure 11. ZnO-based nanocomposites offer a wide range of uses, including the creation of novel materials and the enhancement of well-known parts like sensors, cells, and depositions in terms of quality. Although there are only a few industries that currently use nanocomposites, development from research to industry is accelerating, and in the upcoming years, it is anticipated to be widely used.

Researchers have employed a range of techniques to enhance the ZnO NSs photocatalyst's capacity for efficient removal of organic contaminants as depicted in Fig. 12.

Morphological alterations and crystal defects such distortions and deformation are brought on by doping ZnO. These imperfections in ZnO crystals can significantly enhance the photocatalytic effect when the right doping chemical is added in enough quantity. The amount of doping agent, which depends on the synthesis method and doping agent size, is a crucial factor in boosting visible range photocatalytic action [55]. While keeping ZnO's conduction band and valence band unaltered, metallic dopants offer a new energy band level, and this intra energy band is necessary for specific applications such the creation of large oxidant holes. On the other hand, nonmetallic dopants reduce the band gap while improving the valence band level of ZnO. A metallic dopant can be used to address the major problem of ZnO corrosion when photon energy is present. Inhibition of ZnO growth by metal dopants also leads to the creation of small crystals with a lot of surface area. Based on exploratory and speculative findings, doped ZnO photocatalyst is regarded to be a suitable strategy for enhancing photocatalytic action [56].

Conclusion

Using microwave assisted wet chemical synthesis, rapid synthesis of ZnO NFs of the wurtzite phase has been effectively accomplished in a short synthesis time of 5 minutes. Based on the process of microwave aided wet chemical synthesis, various metal-oxide nanostructures can also emerge. By adjusting the microwave power, microwave time, and kind of precursor solutions, one can change the morphologies, crystal sizes, and crystal growth direction. FESEM and XRD analyses have confirmed the characterizations of the crystalline structure and shape of the produced ZnO NFs. The produced ZnO NFs' crystallite size was calculated using the Scherrer relation and the W-H plot method. Both approaches yield crystallite sizes that fall between 17-19 nm. UV-vis absorption spectrum was used to analyse the optical characteristics of ZnO NFs. The sharp exciton absorbance band near the wavelength of 348 nm is visible in the absorption spectra, and it is validated by the band value of pure ZnO at 353 nm. According to Tauc's approach, the appropriate energy band gap value is 3.22 eV and exhibits a red shift in the wavelength because to the existence of oxygen vacancies. The relationship between the absorption coefficient and photon energy further demonstrates how well the properties match those of semiconducting materials. ZnO NFs' calculated Urbach energy (E_u = 0.34 eV) shows that the materials' micro-structural lattice disorder is present. These characteristics of as-prepared ZnO NFs demonstrate their potential for usage in optoelectronic applications such as electrodes, sensors, emitters, catalysts, and active media. We can draw the conclusion that microwave aided methods can be used to create highly crystalline metal-oxide nanostructures with good semiconducting characteristics for desired applications. The crystalline structure of metal-oxides is preferred for optoelectronic applications, which is obtained in this work; therefore, it can be concluded that this kind of variation indicates the viability of using ZnO NFs for semiconductor device applications.

Declaration of conflicting interests

There is no potential conflict of interest.

Funding

The current work had not received funding of any kind to carry out the study.

Ravi Shankar Rai – Ph.D in Mechanical Engineering, Assistant Professor of the Automation and Robotics Department;
Ruby Pant – Ph.D in Mechanical Engineering, Assistant Professor of the Mechanical Engineering Department;
Shristi Chaudhary – Ph.D in Physics, Assistant Professor of the University Centre for Research and Development;
Rupesh Gupta – Ph.D in Mechanical Engineering, Professor & Director Research at Centre for Research Impact and Outcome;
Chandrmani Yadav – Ph.D in Mechanical Engineering, Assistant Professor (Research) of the Mechanical Engineering Department.

[1] J. Wang, R. Chen, L. Xiang, S. Komarneni, *Synthesis, properties and applications of ZnO nanomaterials with oxygen vacancies: A review*. Ceram Int, 44(7), 7357 (2018); https://doi.org/10.1016/j.ceramint.2018.02.013.
[2] N.A Hammed, A.A Aziz, A.I Usman, M.A Qaeed. *The sonochemical synthesis of vertically aligned ZnO nanorods and their UV photodetection properties: Effect of ZnO buffer layer*. Ultrason Sonochem, 50, 172 (2019); https://doi.org/10.1016/j.ultsonch.2018.09.020.
[3] A. Galdámez-Martinez, G. Santana, F. Güell, PR. Martínez-Alanis, A. Dutt *Photoluminescence of zno nanowires: A review*. Nanomaterials, 10(5), 857 (2020); https://doi.org/10.3390/nano10050857.
[4] T. Blachowicz, A. Ehrmann, *Recent developments in electrospun ZnO nanofibers: A short review.* J Eng Fiber (2020); https://doi.org/10.1177/1558925019899682.
[5] K. Qi, B. Cheng, J. Yu, W. Ho, *Review on the improvement of the photocatalytic and antibacterial activities of ZnO.* J Alloys Compd, 727, 792 (2017); https://doi.org/10.1016/j.jallcom.2017.08.142.
[6] H.H. Azeez, A.A. Barzinjy, S.M. Hamad. *Structure, synthesis and applications of ZnO nanoparticles: A review.* Jordan J Phys, 13(2), 123 (2020); https://doi.org/10.47011/13.2.4.
[7] J. Theerthagiri, S. Salla, R.A. Senthil, P. Nithyadharseni, A. Madankumar, P. Arunachalam, et al. *A review on ZnO nanostructured materials: Energy, environmental and biological applications*. Nanotechnology, 30(39), 392001 (2019); https://doi.org/10.1088/1361-6528/ab268a.
[8] L.J. Chen, Y.C. Chang, J.H. He. *ZnO Nanostructures and Device Applications*. ECS Trans (2019); https://doi.org/10.1149/1.2731176.

[9] C. Li, Q. Hou. *The effects of point defects on the electronic and magnetic properties of GaN/ZnO heterojunction polar interface*. Comput Mater Sci (2019); https://doi.org/10.1016/j.commatsci.2018.10.032.
[10] G. Wang, W. Tang,, L. Geng, Y. Li, B. Wang, J. Chang, et al. *Rotation Tunable Photocatalytic Properties of ZnO/GaN Heterostructures*. Phys Status Solidi Basic Res, 257(3), 1900663 (2020); https://doi.org/10.1002/pssb.201900663.
[11] J. Wang, X. Xi, S. Lin, X. Li, T. Hu, L. Zhao, *Effective photocatalytic water splitting enhancement using GaN/ZnO/NiO core/shell nanocolumns.* J Renew Sustain Energy 13(1), 013702 (2021); https://doi.org/10.1063/5.0035348.
[12] A. Sulciute, K. Nishimura, E. Gilshtein, F. Cesano, G. Viscardi, A.G. Nasibulin, et al. *ZnO Nanostructures Application in Electrochemistry: Influence of Morphology.* J Phys Chem C, 125, 1472 (2021). https://doi.org/10.1021/acs.jpcc.0c08459.
[13] P. Uikey, K. Vishwakarma, *Review of Zinc Oxide (Zno) Nanoparticles Applications and Properties*. Int J Emerg Technol Comput Sci Electron (2016).
[14] R.S. Rai, V. Bajpai, *Recent advances in ZnO nanostructures and their future perspective.* Adv Nano Res (2021); https://doi.org/10.12989/anr.2021.11.1.037.
[15] K. Żelechowska, *Methods of ZnO nanoparticles synthesis*. Biotechnologia, 95(2), 150 (2014); https://doi.org/10.5114/bta.2014.48857.
[16] V. Gerbreders, M. Krasovska, E. Sledevskis, A. Gerbreders, I. Mihailova, E. Tamanis, et al. *Hydrothermal synthesis of ZnO nanostructures with controllable morphology change*. CrystEngComm, 22(8), 1346 (2020); https://doi.org/10.1039/c9ce01556f.
[17] D. Kumar, R.S. Rai, N.K. Singh, *An innovative approach to deposit ultrathin ZnO nanoflakes (2D) through hydrothermal assisted electrochemical discharge deposition and growth method*. Ceram Int; 46, 26216 (2020); https://doi.org/10.1016/j.ceramint.2020.07.009.
[18] K. Edalati, A. Shakiba, J. Vahdati-Khaki, SM. Zebarjad. *Low-temperature hydrothermal synthesis of ZnO nanorods: Effects of zinc salt concentration, various solvents and alkaline mineralizers*. Mater Res Bull, 74? 374 (2016); https://doi.org/10.1016/j.materresbull.2015.11.001.
[19] H.D. Cho, D.Y. Kim, J.K. Lee. *Zno nanorod/graphene hybrid-structures formed on Cu sheet by self-catalyzed vapor-phase transport synthesis*. Nanomaterials, 11(2), 450 (2021); https://doi.org/10.3390/nano11020450.
[20] R.S. Rai, V. Bajpai, *Hydrothermally grown ZnO NSs on Bi-Directional woven carbon fiber and effect of synthesis parameters on morphology*. Ceram Int, (2020); https://doi.org/10.1016/j.ceramint.2020.11.180.
[21] D. Kumar, R.S. Rai, N.K. Singh, *An innovative approach to deposit ultrathin ZnO nanoflakes (2D) through hydrothermal assisted electrochemical discharge deposition and growth method*. Ceram Int (2020); https://doi.org/10.1016/j.ceramint.2020.07.009.
[22] Shankar Rai R. *Carbon fiber fabrics functionalized with monoclinic CuO nanostructures using seed-assisted hydrothermal growth treatment.* Ceram Int; 50, 44635 (2024); https://doi.org/10.1016/J.CERAMINT.2024.08.311.
[23] R.S. Rai, V. Bajpai, *Fabrication of ZnO nanostructures on woven carbon fiber via hydrothermal route and effect of synthesis conditions on morphology*. Int. Conf. Precision, Meso, Micro Nano Eng. IIT Indore, 1 (2019).
[24] S. Baruah, J. Dutta, *Hydrothermal growth of ZnO nanostructures.* Sci Technol Adv Mater; 10 (2009); https://doi.org/10.1088/1468-6996/10/1/013001.
[25] J. Wojnarowicz, T. Chudoba, W. Lojkowski, *A review of microwave synthesis of zinc oxide nanomaterials: Reactants, process parameters and morphoslogies*. Nanomaterials, 10(6), 1086(2020); https://doi.org/10.3390/nano10061086.
[26] H. Sun, L. Sun, T. Sugiura, *White MS, Stadler P, Sariciftci NS, et al. Microwave-assisted hydrothermal synthesis of structure-controlled ZnO nanocrystals and their properties in dye-sensitized solar cells*. Electrochemistry, 85(5), 253 (2017); https://doi.org/10.5796/electrochemistry.85.253.
[27] N. Senthilkumar, E. Vivek, M. Shankar, M. Meena, M. Vimalan, I.V. Potheher. *Synthesis of ZnO nanorods by one step microwave-assisted hydrothermal route for electronic device applications.* J Mater Sci Mater Electron, 29(4), (2018); https://doi.org/10.1007/s10854-017-8223-5.
[28] V. Musat, A. Filip, N. Tigau, R. Dinica, E. Herbei, C. Romanitan, et al. *1D nanostructured ZnO layers by microwave - Assisted hydrothermal synthesis.* Rev Chim, (2018); https://doi.org/10.37358/rc.18.10.6625.
[29] Z. Zhu, D. Yang, H. Liu, *Microwave-assisted hydrothermal synthesis of ZnO rod-assembled microspheres and their photocatalytic performances*. Adv Powder Technol, 22, 493 (2011); https://doi.org/10.1016/j.apt.2010.07.002.
[30] K.R. Ahammed, M. Ashaduzzaman, S.C. Paul, M.R. Nath, S. Bhowmik, O. Saha, et al. *Microwave assisted synthesis of zinc oxide (ZnO) nanoparticles in a noble approach: utilization for antibacterial and photocatalytic activity*. SN Appl Sci, 2(95), (2020); https://doi.org/10.1007/s42452-020-2762-8.
[31] M. Yalcin, *Microwave-assisted synthesis of ZnO nanoflakes: Structural, optical and dielectric characterization.* Mater Res Express, 7(5), (2020). https://doi.org/10.1088/2053-1591/ab940f.
[32] D. Sharma, S. Sharma, B.S. Kaith, J. Rajput, M. Kaur, *Synthesis of ZnO nanoparticles using surfactant free in-air and microwave method.* Appl Surf Sci, 257(22), 9661 (2011); https://doi.org/10.1016/j.apsusc.2011.06.094.

[33] R. Al-Gaashani, S. Radiman, A.R. Daud, N. Tabet, Y. Al-Douri, *XPS and optical studies of different morphologies of ZnO nanostructures prepared by microwave methods*. Ceram Int; 39, 2283 (2013); https://doi.org/10.1016/j.ceramint.2012.08.075.

[34] D. Kumar, R.S. Rai, V. Bajpai, N.K. Singh. *Mass fabrication of 2D nanostructure (ZnO) in chemical growth solution using tip induced lithography.* Mater Manuf Process; 1 (2021); https://doi.org/10.1080/10426914.2021.1960993.

[35] J.W. Nowak, R.S.W. Braithwaite, J. Nowak, K. Ostojski, M. Krystek, W. Buchowiecki, *Formation of large synthetic zincite (ZnO) crystals during production of zinc white.* J Gemmol, 30(5), 257 (2007); https://doi.org/10.15506/jog.2007.30.5.257.

[36] H. Shelton, M.C. Barkley, R.T. Downs, R. Miletich, P. Dera, *Hydrogen bond effects on compressional behavior of isotypic minerals: high-pressure polymorphism of cristobalite-like Be(OH)2.* Phys Chem Miner 43(8), 571 (2016); https://doi.org/10.1007/s00269-016-0818-5.

[37] K. Ocakoglu, S.A. Mansour, S. Yildirimcan, A.A. Al-Ghamdi, F. El-Tantawy, F. Yakuphanoglu, *Microwave-assisted hydrothermal synthesis and characterization of ZnO nanorods*. Spectrochim Acta - Part A Mol Biomol Spectrosc,148, 362 (2015); https://doi.org/10.1016/j.saa.2015.03.106.

[38] I Ben Saad, N. Hannachi, T. Roisnel, F. Hlel, *Optical, UV-Vis spectroscopy studies, electrical and dielectric properties of transition metal-based of the novel organic-inorganic hybrid (C6 H10 N2)(Hg2Cl5)2.3H2O.* J Adv Dielectr, (2019); https://doi.org/10.1142/S2010135X19500401.

[39] Bhawna, Roy M, Vikram, Borkar H, Alam A, Aslam M. *Spontaneous anion-exchange synthesis of optically active mixed-valence Cs2Au2I6perovskites from layered CsAuCl4perovskites.* Chem Commun (2021); https://doi.org/10.1039/d0cc06922a.

[40] A.H. Moharram, S.A. Mansour, M.A. Hussein, M. Rashad, *Direct precipitation and characterization of ZnO nanoparticles*. J Nanomater, 2014(7), (2014); https://doi.org/10.1155/2014/716210.

[41] A. Elkhidir Suliman, Y. Tang, L. Xu, *Preparation of ZnO nanoparticles and nanosheets and their application to dye-sensitized solar cells*. Sol Energy Mater Sol Cells (2007); https://doi.org/10.1016/j.solmat.2007.05.014.

[42] S. Zandi, P. Kameli, H. Salamati, H. Ahmadvand, M. Hakimi, *Microstructure and optical properties of ZnO nanoparticles prepared by a simple method.* Phys B Condens Matter, 406, 3215 (2011); https://doi.org/10.1016/j.physb.2011.05.026.

[43] M. Kahouli, A. Barhoumi, A. Bouzid, A. Al-Hajry, S. Guermazi, *Structural and optical properties of ZnO nanoparticles prepared by direct precipitation method.* Superlattices Microstruct, 85, 7 (2015); https://doi.org/10.1016/j.spmi.2015.05.007.

[44] A. Bougrine, A. El Hichou, M. Addou, J. Ebothé, A. Kachouane, M. Troyon, *Structural, optical and cathodoluminescence characteristics of undoped and tin-doped ZnO thin films prepared by spray pyrolysis.* Mater Chem Phys, 80(2), 438 (2003); https://doi.org/10.1016/S0254-0584(02)00505-9.

[45] M. Caglar, S. Ilican, Y. Caglar, F. Yakuphanoglu, *Electrical conductivity and optical properties of ZnO nanostructured thin film*. Appl Surf Sci, 255, 4491(2009); https://doi.org/10.1016/j.apsusc.2008.11.055.

[46] G. Poongodi, P. Anandan, R.M. Kumar, R. Jayavel, *Studies on visible light photocatalytic and antibacterial activities of nanostructured cobalt doped ZnO thin films prepared by sol-gel spin coating method*. Spectrochim Acta - Part A Mol Biomol Spectrosc, 5(148), 237(2015); https://doi.org/10.1016/j.saa.2015.03.134.

[47] M. Wang, F. Ren, J. Zhou, G. Cai, L. Cai, Y. Hu, et al. *N Doping to ZnO Nanorods for Photoelectrochemical Water Splitting under Visible Light: Engineered Impurity Distribution and Terraced Band Structure.* Sci Rep, 5(1), 12925 (2015); https://doi.org/10.1038/srep12925.

[48] D. Panda, T.Y. Tseng. *One-dimensional ZnO nanostructures: Fabrication, optoelectronic properties, and device applications*. J Mater Sci, 48(20), 6849 (2013); https://doi.org/10.1007/s10853-013-7541-0.

[49] K. Kong, J. Seo, B.K. Deka, H.W. Park, Experimental study for the improvement of the impact property of carbon fiber composites, 1641 (2015).

[50] X. Wang, M. Ahmad, H. Sun, *Three-dimensional ZnO hierarchical nanostructures: Solution phase synthesis and applications*. Materials (Basel), 10, 1 (2017); https://doi.org/10.3390/ma10111304.

[51] N. Zheng, Y. Huang, W. Sun, X. Du, H.Y. Liu, S. Moody, et al. *In-situ pull-off of ZnO nanowire from carbon fiber and improvement of interlaminar toughness of hierarchical ZnO nanowire/carbon fiber hydrid composite laminates*. Carbon N Y, 110 (10), 69 (2016); https://doi.org/10.1016/j.carbon.2016.09.002.

[52] G.J. Ehlert, U. Galan, H.A. Sodano. *Role of surface chemistry in adhesion between ZnO nanowires and carbon fibers in hybrid composites*. ACS Appl Mater Interfaces, 5(3), 635 (2013); https://doi.org/10.1021/am302060v.

[53] H. Moussa, E. Girot, K. Mozet, H. Alem, G. Medjahdi, R. Schneider, *ZnO rods/reduced graphene oxide composites prepared via a solvothermal reaction for efficient sunlight-driven photocatalysis*. Appl Catal B Environ, 185, 11 (2016); https://doi.org/10.1016/j.apcatb.2015.12.007.

[54] T.S. Velayutham, W.H. Abd Majid, W.C. Gan, A. Khorsand Zak, S.N. Gan. *Theoretical and experimental approach on dielectric properties of ZnO nanoparticles and polyurethane/ZnO nanocomposites*. J Appl Phys 112(101), (2012); https://doi.org/10.1063/1.4749414.

[55] Y. Chen, Y. Wang, J. Fang, B. Dai, J. Kou, C. Lu, et al. *Design of a ZnO/Poly(vinylidene fluoride) inverse opal film for photon localization-assisted full solar spectrum photocatalysis.* Chinese J Catal, 42(1), 184 (2020); https://doi.org/10.1016/S1872-2067(20)63588-4.

[56] H. Deng, F. Xu, B. Cheng, J. Yu, W. Ho, *Photocatalytic CO_2 reduction of C/ZnO nanofibers enhanced by an Ni-NiS cocatalyst*. Nanoscale, 12, 7206 (2020); https://doi.org/10.1039/c9nr10451h.

Раві Шанкар Рай[1]*, Рубі Пант[2], Шріші Чаудхарі[3], Рупеш Гупта[4], Чандрмані Ядав[5]

Синтез та характеристика наноквітів ZnO для оптоелектроніки, отриманих одностадійним мікрохвильовим сольвотермальним методом

*[1]*Кафедра автоматизації та робототехніки, Інженерний коледж Раджарші Шаху (JSPM), Пуна, Махараштра, Індія, rash.mait@gmail.com;*
[2]Кафедра машинобудування, Університет Уттаранчал, Деградун, Уттаракханд, Індія;
[3]Університетський центр досліджень і розробок, Університет Чандігарх, Гаруан, Пенджаб, Індія;
[4]Інститут інженерії та технологій Університету Чіткара, Університет Чіткара, Пенджаб, Індія;
[5]Дослідницький центр Університету Марваді, факультет інженерії та технологій, кафедра машинобудування, Університет Марваді, Раджкот, Гуджарат, Індія

У даному дослідженні було синтезовано квіткоподібні нанокристали ZnO (наноквіти) швидким одностадійним мікрохвильовим сольвотермальним методом із використанням гексагідрату нітрату цинку та гексаметилентетраміну, як прекурсорів. Синтез тривав п'ять хвилин, здійснювався із застосуванням недорогих реагентів та без використання високотемпературних печей, що забезпечує ефективний та економічно доцільний підхід. Структурний аналіз методом Х-променевої дифракції підтвердив високу кристалічність наноквітів ZnO, тоді як скануюча електронна мікроскопія з польовою емісією виявила їх характерну квіткоподібну морфологію із середнім розміром частинок близько 18 нм. Оптичні властивості досліджувалися методом УФ-видимої спектроскопії; чіткий максимум поглинання поблизу 348 нм свідчить про добру монодисперсність. Оптична ширина забороненої зони, визначена за співвідношенням Таука, становить 3,22 еВ, що є суттєво меншим значенням, порівняно із масивним ZnO (3,51 еВ) та вказує на червоне зміщення. Обчислена енергія Урбаха (0,34 еВ) свідчить про низький рівень структурної невпорядкованості в наноструктурах. Поєднання швидкого синтезу, контрольованої морфології, високої кристалічності та сприятливих оптичних характеристик підкреслює новизну та значний потенціал наноквітів ZnO для перспективних оптоелектронних і фотонних пристроїв.

Ключові слова: мікрохвильове опромінення, сольвотермальний метод, синтез, ZnO, наноквіти, оптоелектроніка